Biogeosciences Discuss., 6, 825–862, 2009
www.biogeosciences-discuss.net/6/825/2009/

Biogeosciences Discussions

Biogeosciences Discussions is the access reviewed discussion forum of *Biogeosciences*

Estimation of NH_3 emissions from a naturally ventilated livestock farm using local-scale atmospheric dispersion modelling

A. Hensen[1], B. Loubet[2], J. Mosquera[1,*], W. C. M. van den Bulk[1], J. W. Erisman[1], U. Dämmgen[3], C. Milford[4], F. J. Löpmeier[3], P. Cellier[2], P. Mikuška[5], and M. A. Sutton[4]

[1]The Energy research Centre of the Netherlands (ECN), Petten, The Netherlands
[2]Institut National de la Recherche Agronomique (INRA), Thiverval-Grignon, France
[3]Federal Agricultural Research Centre, Braunschweig (FAL), Germany
[4]Centre for Ecology and Hydrology (CEH), Edinburgh, UK
[5]Institute of Analytical Chemistry, ASCE, v.v.i., Brno, Czech Republic
[*]now at: Animal Sciences Group (ASG), Wageningen, The Netherlands

Received: 11 September 2008 – Accepted: 14 November 2008 – Published: 14 January 2009

Correspondence to: A. Hensen (hensen@ecn.nl)

Published by Copernicus Publications on behalf of the European Geosciences Union.

Abstract

Agricultural livestock represents the main source of ammonia (NH_3) in Europe. In recent years, reduction policies have been applied to reduce NH_3 emissions. In order to estimate the impacts of these policies, robust estimates of the emissions from the main sources, i.e. livestock farms are needed. In this paper, the NH_3 emissions were estimated from a naturally ventilated livestock farm in Braunschweig, Germany during a joint field experiment of the GRAMINAE European project. An inference method was used with a Gaussian-3-D plume model and a local-scale dispersion and deposition model (FIDES-2-D). NH_3 concentrations downwind of the source were used together with micrometeorological data to estimate the source strength over time. Mobile NH_3 concentration measurements provided information on the spatial distribution of source strength. The estimated emission strength ranged between 6.0±0.17 kg NH_3 d^{-1} (FIDES-2-D model) and 9.2±0.7 kg NH_3 d^{-1} (Gaussian model). These estimates were 94% and 63% of what was obtained using emission factors from the German national inventory (9.6 kg d^{-1} NH_3). However, the FIDES-2-D approach was shown to be very sensitive to the source size, the roughness height and to whether deposition was taken into account downwind of the source. Accounting for deposition in FIDES-2-D gives a potential emission estimate of 11.7 kg NH_3 d^{-1}, showing that deposition can explain the observed difference. The daily pattern of the source was correlated with net radiation and with the temperature inside the animal houses. The daily pattern resulted from a combination of a temperature effect on the source concentration together with an effect of variations in free and forced convection of the building ventilation rate. Further development of the plume technique is especially relevant for naturally ventilated farms, since the variable ventilation rate makes other emission measurements difficult.

BGD

6, 825–862, 2009

1 Introduction

Atmospheric ammonia (NH_3) is recognised as a major pollutant impacting on sensitive ecosystems (Bobbink et al., 1992). NH_3 deposition may indeed cause soil acidification through nitrification processes (van Breemen et al., 1982), although this depends upon the biological and chemical status of the soil on which it is deposited, and upon the form of NH_x deposited (NH_3 or NH_4^+) (Galloway, 1995). Furthermore, atmospheric inputs of NH_x may induce eutrophication of sensitive ecosystems, as well as decrease their biodiversity (Heij and Schneider, 1991; Bobbink et al., 1992). Agriculture is the main source of NH_3 in Europe (Asman, 1992; Heij and Schneider, 1995), and represents more than 80% of the total anthropogenic input at the global scale (Bouwman et al., 1997). The inventory studies of Jarvis and Pain (1990), of Pain et al. (1998) and Döhler et al. (2002) show that cattle represents the largest source of agricultural NH_3 emissions in Europe. These studies as well as Bussink et al. (1998) also showed that between 40% and 50% of the emissions from cattle arise from housing and waste storage, housing itself representing about 7% to 10%. There are also important emissions from pig and poultry production, although the emission factor per animal is smaller for these animals.

Measurement of NH_3 emissions from naturally ventilated animal houses is technically complex, expensive, and labour intensive (Phillips et al., 2001; Scholtens et al., 2004; Welch et al., 2005a, b). This is primarily due to difficulties in determining the ventilation rate, which varies according to temperature, wind speed, building design, orientation to the wind and animal occupancy (Zhang et al., 2005; Welch et al., 2005b), but also to difficulties inherent in accurately measuring the ammonia concentration on short-time basis (Phillips et al., 2005). However, methods such as the internal or external tracer-ratio techniques or the flux-sampling technique have been successfully tested under real conditions (Demmers et al., 2001; Dore et al., 2004).

Dispersion models can be used as tools to estimate ammonia emissions from animal houses. Among them, the Gaussian plume model, assuming constant wind-speed (U)

and diffusivity (Kz) with z is widely used because of its simplicity (Gash, 1985). Analytical models that include variation of U and Kz with height also exist (e.g., Smith, 1957; Philip, 1959; Yeh and Huang, 1975; Huang, 1979; Wilson et al., 1982). The technique using Gaussian models to infer NH_3 source from a farm building has been reported in Mosquera et al. (2004). Lagrangian stochastic models have also been tested to infer sources of tracers from concentration measurements downwind of sources such as animal houses (Flesch et al., 2005) cattle feedlots (Flesch et al., 2007), and fields (Loubet et al. 2006; Sommer et al., 2005). More complex Eulerian models have also been used and validated against extensive measurements for estimating emissions of NH_3 from buildings (Welch et al., 2005b).

In this paper, a Gaussian-3-D plume model and a 2-D dispersion model (FIDES-2-D, Loubet et al., 2001) are used to estimate the source strength of a set of farm buildings in an experimental field site in Braunschweig (Germany). The stationary measurements of ammonia concentrations were used to infer the source strength of several farm buildings upwind. The inferred emissions are compared with inventory emission factors. The daily variability of the emissions is analysed in comparison with environmental factors such as indoor temperature, external radiation and wind speed. The inferred emission strengths are used in a companion paper (Loubet et al., 2006) as inputs for quantifying the local advection errors induced by the plume coming from the farm on NH_3 fluxes measured over a grassland site nearby. This study was performed within the framework of the European project GRAMINAE.

2 Materials and methods

2.1 Measurement site

The field site is a 12 ha experimental grassland situated in the grounds of the Federal Agricultural Research Centre (FAL), Braunschweig, Germany. Directly adjacent to the field are an experimental farm of the FAL and a station of the German Weather Service

(Deutscher Wetterdienst). A more detailed description of the site can be found in Sutton et al., 2008. The main source of ammonia in the area is the set of farm buildings A-K (Fig. 1). The distance from west to east is named x, whereas the distance from south to north is called y, and height above ground is z. The distance between the downwind edge of the farm building area and the different sites are: 230 m for site 3, 610 m for site 1, and 810 m for site 2. The farm buildings themselves occupy an area of approximately 180 m (E-W)×200–300 m (S-N). The defined area of the source is essential in this study, since the area was applied in the two-dimensional approach to define an equivalent two-dimensional source, as well as to scale the total emission of the source, knowing the source strength. In the three-dimensional approach, the (x, y) co-ordinates of the sources and the receptors were directly used in the model. Table 1 gives an estimate of the yearly NH_3 emission for each building identified in Fig. 1, based on the emission factors of Döhler et al. (2002). As a comparison, measurement-based estimates of Demmers et al. (2001) in Great-Britain are 3.5 and 8.9 kg NH_3 per animal per year, for beef and dairy cattle, respectively.

2.2 Concentration measurements

The locations of ammonia concentration measurements are shown as grey dots in Fig. 1. Three Amanda rotating wet denuders (Wyers et al., 1993) were placed along the N-S transect at Site 3, which gave NH_3 concentrations on a 30 min averaging period at 1 m height. These instruments were also used to calibrate a fast-response mobile NH_3 analyser, itself being moved along the North-West line on the adjacent track (marked as Site 3 in Fig. 1), to measure the plume cross-section at 1.5 m height. At Site 1, NH_3 concentrations were measured using three independent AMANDA systems giving the vertical fluxes and concentration over a 15 min period Milford et al., 2008. At Site 2, fluxes and concentration were measured with a single gradient-AMANDA system. At Sites 1 and 2, the concentration estimates for 1 m height were used in this study. The background NH_3 concentrations were measured with a batch denuder system, located at 42 m height on the top of a tower (Site 6 in Fig. 1), which was located 800 m North-

East of the grassland. Mean and standard deviation of the concentration was estimated for Sites 1 and 3 over the three measurement systems.

For the mobile measurements, a fast response AMANDA sensor was used, with a time resolution of 30 s. This system, described in Erisman et al. (2001), is essentially similar to an AMANDA, but the liquid flow is higher (10 ml min^{-1} instead of 1.6 ml min^{1}). However, it does not give an absolute concentration, and therefore requires regular calibrations against a reference. The fast response sensor was placed on a trolley and moved along a track through the plume cross-section, and calibrated against the three AMANDA sensors on the same transect (Fig. 1). Note that the calibration was done on differing integration time, as the AMANDA integrates over 15 min. The location of the fast response sensor was calculated as a function of time. Four subsequent transects were used to evaluate the emission with these data.

2.3 Micrometeorological measurements

Micrometeorological measurements were performed at Sites 1 and 2. The consensus micrometeorological database derived from the range of measurements performed and detailed in Nemitz et al., 2008 was used in this study. The wind-speed (U), wind-direction (WD), friction velocity (u_*), Monin-Obukhov length (L), and sensible heat fluxes (H), were derived from several ultrasonic anemometer measurements. The latent heat flux (LE) was derived from eddy covariance measurements using the ultrasonic anemometers in combination with a close-path H_2O analyser (Licor 6262) or open-path H_2O analyser (KH_2O). Air temperature (T_a), relative Humidity (HR) and global (R_g) and net radiation (R_n) were also used.

3 Inference of the source strength from NH_3 concentration

3.1 General approach

NH_3 concentrations as measured with the systems described above, were used to infer the source strength using backward dispersion modelling, and micrometeorological parameters. Using a single dispersion model, many inference methods could be used, and on the contrary, with one inference method, many dispersion models could be used. In this paper, we compare two models: a 3-D Gaussian plume model that assumes a constant wind speed (U) and diffusivity (K_z) everywhere and the FIDES-2-D model that assumes that both U and K_z are power low functions of height, but assumes homogeneity in the crosswind direction (see Loubet et al., 2001, for details).

Three inference methods were used to estimate the source strength:

1. The Gaussian-3-D model was used in conjunction with mobile NH_3 measurements to estimate the source strength, based on a source distribution equivalent to the emission inventory.

2. The Gaussian-3-D model was used in conjunction with concentrations measured at the three locations of Site 3 to estimate the spatial distribution of the source using wind-direction changes.

3. The FIDES-2-D and the Gaussian-3-D model were used in conjunction with 15 min NH_3 concentration measured at Site 3 to estimate the variation in time of the source, knowing its spatial variability.

The basic hypothesis made in these approaches are: (a) unless specified, no NH_3 deposition is included, as it is considered to be of secondary importance compared with the effect of dispersion on the concentration (e.g., Loubet and Cellier, 2002); (b) no chemical reactions are envisaged, as again the effect on the overall NH_3 concentration is not expected to be large on such a small scale (Nemitz et al., 2008); and (c)

the surface characteristics are considered to be homogeneous (i.e., z_0, d), since the models used cannot deal with varying surface roughness, though this is considered to be of minor importance regarding the uncertainty linked with the modified flow around the buildings.

With each of the models, the approach is based on the general superposition principle (e.g., Thomson, 1987; Raupach, 1989), which relates the concentration at a location (x, y, z), $\chi(x, y, z)$, to the source strength at another location (x_s, y_s, z_s), $S(x_s, y_s, z_s)$, with the use of a dispersion function $D(x, y, z/x_s, y_s, z_s)$ (in s m^{-}3):

$$\chi(x,y,z) = \chi_{\text{bgd}} + \int_{\text{all } x_s \text{ and } y_s} S(x_s,y_s,z_s) D(x,y,z|x_s,y_s,z_s) dx_s \quad (1)$$

where χ_{bgd} is the background concentration, assumed to be constant with height, and fixed to the concentration at Site 6. The two models are different in the way they calculate the dispersion function $D(x, y, z| x_s, y_s, z_s)$ and the different approaches are detailed in the following.

3.2 The Gaussian plume model

The Gaussian plume model is based on the assumptions that U and K_z are constant in the whole domain, which implies that $\chi(x, y, z)$ is a function of two independent Gaussian distributions in the horizontal and the vertical planes (see e.g. Lin and Hildemann, 1997). The contribution from a single source located at (x_s, y_s, z_s) to a point receptor located at (x, y, z) is the dispersion function $D(x, y, z/ x_s, y_s, z_s)$, which was calculated using $X = x - x_s$ and $Y = y - y_s$, as:

$$D(X,Y,z) = \frac{Q}{2\pi \cdot \sigma_y \cdot \sigma_z} \cdot e^{-Y^2 / (2\cdot\sigma_y)^2} \cdot \left(e^{-(z-h_s)^2 / (2\cdot\sigma_z)^2} + e^{-(z+h_s)^2 / (2\cdot\sigma_z)^2} \right) \quad (2)$$

$$\sigma_y = a \cdot X^b \cdot z_o^{0.2} \cdot T^{0.35}$$
$$\sigma_z = c \cdot X^d \cdot (10 \cdot z_o)^{0.53 \cdot e} \quad (3)$$
$$e = X^{-0.22}$$

where Q is the source strength (in g s^{-1} NH_3), h_s the height of the source (animal house) (in m), σ_y and σ_z are the standard deviation of the lateral and vertical concentration distribution respectively (in m), z_o is the roughness length (in m), T is the averaging time, and the parameters a, b, c and d are dependent on the stability classes as detailed in Pasquill (1974). The model used is a multiple plume model based on the superposition of several Gaussian plumes each described by Eq. (2–3). The concentration at each receptor is the sum of the contribution of all the sources according to (1). The downwind (X) and crosswind (Y) distances are calculated for each source-receptor couple as follows:

$$X = -(x(R) - x(S)) \cdot \sin(WD) - (y(R) - y(S)) \cdot \cos(WD)$$
$$Y = (x(R) - x(S)) \cdot \cos(WD) - (y(R) - y(S)) \cdot \sin(WD) \quad (4)$$

where $(x(R), y(R))$ and $(x(S), y(S))$ are the receptor and source coordinates, respectively.

3.3 The fidess-2-D model

In this two-dimensional model, $D(x, z/x_s, z_s)$ was estimated using the Huang (1979) semi-analytical dispersion model, based on the use of power law functions to describe $U(z)$ and $K_z(z)$. A description and evaluation of the dispersion model is given in Loubet et al. (2001). In this model, the stability corrections are calculated using the Monin-Obukhov length. Since FIDES-2-D is a two-dimensional (2-D) model, an equivalent 2-D sketch needs to be drawn. This is done by considering that the source was a homogeneous area of width 180 m in x and infinite in y. This is a valid assumption for a limited wind direction sector. With a north-south extension of the farm of 300 m and a receptor at 230 m downwind of the site, a winds-sector of ± 30 degrees around

the wind-direction of the centre of the farm (when observed from site 3, 270°) was chosen. In order to estimate the source strength in g s^{-1} NH_3, the source strength per unit area inferred by FIDES-2-D has been multiplied by the equivalent surface of the source: 180 m×300 m. The model has the possibility to take deposition downwind of the source into account; it is applied without dry deposition apart from where stated in the text. As the model uses stability corrections (Kaimal and Finnigan, 1994), its use is limited to values of the Monin Obukhov length (L) and the friction velocity u_* such that $|L|$>5 m and u_*> 0.2 m s^{-1}.

3.4 Estimate of the spatial distribution of the source with the Gaussian 3-D model

The Gaussian plume model was used in backward mode to infer the source strength of the farm buildings, using the ammonia concentration measured at the three fixed points at Site 3 ($AM_{1..3}$). The procedure consisted in using the Gaussian model in forward mode to estimate the contribution to concentration at the 3 receptor locations for each of the 11 source locations in Table 1. For each receptor location the measured concentration at time T is compared with the sum of the 11 model runs at the same time T. Modification of the relative importance of the 11 sources was simulated by multiplication of each model time series with a coefficient. These coefficients were changed using the EXCEL (Microsoft) solver function in order to optimise the correlation coefficient between the measured and modelled concentration time series. All sources strengths were assumed constant with time. The emission strength of the whole farm area S_{farm} was calculated for each 15 min measurement interval t at the individual receptor locations ($AM_{1..3}$) using :

$$S_{farm}(t, AM_i) = Q_{input} \times \frac{\chi_{measured}(AM_i) - \chi_{bgd}}{\chi_{model}(AM_i)} \quad (5)$$

where Q_{input} is the initial source strength used to estimate χ_{model}, AM_i=(AM_1, AM_2 or AM_3) is the receptor location at Site 3. The time-average and standard deviation of

S_{farm} was then estimated at each receptor locations $AM_{1..3}$. Since these locations are between the farm and the main field the emission from the farm site were evaluated using all measurements with a wind direction between 200° and 340°.

3.5 Time evolution of the source strength

The FIDES-2-D model was used in a backward mode to estimate the source strength as a function of time. For that, the concentration at Site 3, averaged over the three sensors was used, and one area source was considered of size 180 m×300 m. $D(x,z)$ was calculated using FIDES-2-D, and Eq. (1) was inverted giving $S=(\chi(x)-\chi_{bgd})/D(x,z)$. The Gaussian-3-D model was used similarly to estimate $S=(\chi\ (X,Y)-\chi_{bgd})/D(X,Y,z)$. The wind sector considered was 240°–300°, which corresponds to a sector of ± 30° around the average wind direction as discussed in Sect. 3.3.

4 Results

4.1 Spatial variability of the source illustrated with the fast response NH_3 sensor

Figure 2 shows two NH_3 concentration transects across the plume coming from the farm, obtained with the fast response sensor at Site 3. The transects were obtained at midday from 12:00 to 14:00 on 12 June. The absolute concentration differs slightly between the two periods, which could be explained on the basis of differences in windspeed.

Four plumes obtained with the mobile measurements system were used to evaluate the emission of the farm site. A set of two model runs was performed using the source distribution in Table 1. The potential for large and small initial mixing close to the farm area was evaluated by setting an initial horizontal dispersion at the farm source of either 50 or 10 m. Initial dispersion in the vertical direction was set to 5 m. The two model runs provide concentration patterns along the transect that were compared with

the measured concentration levels. The source estimates for the four plumes and two model runs are shown in Table 2. The emission needed in the model to make the output fit with the measurements is about 10% higher for the plumes 2–4 compared with the inventory source strength. Including plume 1, the emission estimate equals the inventory estimate at 9.6 kg NH_3 d^{-1}.

The mobile plume measurements show the shape of the plume providing information on the lateral dispersion. The model runs for these plumes showed that the lateral dispersion in the model corresponds with the measurement data at a roughness length z_o=0.2 m. The mobile measurements only covered a small time-period and were hard to do during the night. Therefore, the spatial distribution of the sources within the farm area was evaluated further using the three AMANDA stations AM_1-AM_3 at Site 3. Using the source distribution of Table 1 (emission inventory), and tuning the overall source strength S_{fam}, the modelled and measured concentration patterns for the three AMANDA locations showed low correlation coefficients of R=0.36, 0.30 and 0.20 respectively (Table 3). The model calculations were used to obtain insight in the source-receptor relation for each measurement location. Sources A, B, D and F give the highest contribution to the modelled signal at the three receptor locations. The time series of the estimated S_{farm} (Eq. 5) were used to estimate the average, standard deviation and median (Table 3). The average emission level obtained in this way was 9.8±0.8 kg NH_3d^1, which is close to the expected level of 9.6 kg NH_3d^1. The uncertainty range of 0.8 kg NH_3 d^{-1} was obtained from the standard errors in Table 3. The standard deviation of the source estimate is about 100% this is a combination of uncertainty in the method and of the actual temporal variation of the source strength (discussed below).

In a second step, the correlation between the measured and modelled concentration pattern at Site 3 was optimised by modifying the source distribution. The results are shown in Table 4. The source distribution estimated by this means shows a decreased contribution from sources A, E and F, and an increase in the emission from B and C. The correlation between measured and modelled concentration patterns increased to

BGD
6, 825–862, 2009

R=0.5 and 0.49 for stations AM1 and AM2. No significant effect is observed for AM3. The revised total source strength estimate obtained from the time-series at this source distribution is 9.2 kg $NH_3 d^{-1}$. Accounting for simple uncertainty in estimates by system AM1-3 (n=3) gives a standard error of 1.6 kg NH_3 d^{-1}, which gives a conservative estimate of the uncertainty. Conversely, given the large sample sizes (n=286 to 441), standard errors for the individual AMANDA systems are in the range 0.2–0.6 kg NH_3 d^{-1}.

Figure 3 shows an illustration of the measured and modelled concentrations using the Gaussian-3-D model for AM1-3 at Site 3 over a two-day period using the adjusted source distribution. The correlation coefficient in Table 4 shows that 10–25% of the temporal variation can be explained. The differences are expected to be due to the assumption of a constant source-strength with time. This shows that the combination of time variation in meteorological conditions and the spatial variability of the source can explain part of the variability in the concentration, but not all.

Table 5 gives the estimated source strength using the Gaussian plume model, as well as the source strength estimated using the emission factors of Döhler et al. (2002). The modification in the source distribution, which was done in order to increase the correlation between measurements and model, suggests that the sources in the south have a low emission, whereas the sources in the north are a factor 3–5 higher. For building A,E,G the Gaussian plume model significantly underestimates the relative source strength, whereas it overestimates for buildings C,D, I, and K.

4.2 Temporal variability of the source estimated from backward modelling with fides-2-D

Figure 4 shows an example result of inferred source strength (kg NH_3 day^{-1}) using the FIDES-2-D model for the windsector 240°–300°. Hourly values of the source strength varied from 0 to 800 g h^{-1} NH_3 during the whole period. Figure 4 shows a clear diurnal variation with a maximum emission at midday and a minimum during the night.

This daily variability is not always due to concentration change, as shown by the example shown in Fig. 4 (bottom graph) where concentration difference χ-χ_{bgd} is constant and the source strength varies. The variability is also due to the turbulent diffusivity increasing during the day, therefore requiring a larger source to generate a similar concentration at a given distance. Averaging the inferred hourly emission rates over all the available data (for westerly winds), and converting to daily emission rates lead to an average emission of 6.0 kg d^{-1} NH_3, with a standard error of 0.17 kg d^{-1} NH_3 (N=512).

The inferred emission strength was averaged to hourly values in order to estimate a mean daily pattern (Fig. 5). The daily pattern was observed throughout the period, with a minimum between 01:00 and 02:00 GMT in the morning and a maximum between 07:00 and 09:00 GMT in the morning, then decreasing towards the end of the day. This pattern is partly reflected by the concentration difference between Site 3 and the background concentration, also shown in Fig. 5. Note that there are not many data at night, due to u_* or $|L|$ being below the model requirement under stable conditions, so that the results obtained for night-time conditions are less certain than for the day.

5 Discussion

5.1 Emissions from the farm buildings estimated with different techniques and sensitivity analysis

The averaged daily emission estimated with the Gaussian plume model was found to be 9.2±0.7 kg d^1 NH_3, 6.0±0.17 kg d^{-1} (± standard errors) NH_3 as estimated with the FIDES-2-D model and 9.6 kg d^{-1} NH_3 as estimated by the emission factors. The inferred emission strength with the Gaussian plume and the FIDES-2-D model would represent 3.3 tonnes NH_3 $year^{-1}$ and 2.1 tonnes NH_3 $year^1$, respectively. Although, the inventory emission factors do not include formal uncertainty estimates, the comparison with the estimates of Demmers et al. (2001) for dairy cattle of 8.9 kg NH3 $animal^{-1}$ yr^{-1} compared with 10.35 kg $animal^{-1}$ yr^{-1} of Döhler et al. (2002) suggests that the

difference between the Gausian plume estimates and the inventory (5%) is within the range of uncertainties. Conversely, the FIDES-2-D model, using the parametrization applied was 35% lower than the inventory and Gaussian model estimates.

Underestimation of emissions by such models has been observed before. For example, Welch et al. (2005b) found a collection efficiency of 80% using the ADMS model in a controlled NH_3 release experiment. However, Flesch et al. (2004) found a much better collection efficiency with a methane tracer using a backward Lagrangian Stochastic model under flat terrain conditions. Flesch et al. (2004) also showed that the modelling approach was not reliable under strongly stratified conditions. Michorius et al. (1997) evaluated that the underestimation of NH_3 emission by a farm building using a Gaussian plume approach and concentrations measured at 100 m varied from 47% to 68% of the expected emission. Such small estimates from the models as compared to the emission factors could be due to:

1. a small sampling time due to the concentration measurements being done only on the east of the farm, which may hence induce a bias if wind direction show a daily pattern. This was indeed the case as the wind was blowing from the west 7% of the time at 15:00 and only 1.5% of the time at 05:00. However, this would lead to a bias toward higher emission estimates.

2. the measured NH_3 concentration at 230 m downwind from the farm being lowered by the dry deposition taking place between the farm buildings and Site 3. This hypothesis was tested in a sensitivity analysis using FIDES-2-D (see Table 3 and discussion below).

3. the FIDES-2-D model not taking into account the lateral dispersion, hence giving larger concentrations for a same source strength at a downwind distance which is of the same order as the width of the source. This certainly explains why the FIDES-2-D gives lower estimates of the source strengths as compared to the Gaussian plume model.

4. the experimental farm being especially well managed with surfaces regularly cleaned of manure, so that the emission factors estimated from national inventories might not apply here.

The uncertainty ranges reported for the source strength estimate based on the Gaussian model of about 10–15% were calculated from the standard errors in the three calculated timeseries. A sensitivity analyses for the different inputs required in the Gaussian model calculation showed a 10% effect for a change of 50% in the z_o values used. Changing the source height from 4 to 10 m would decrease the emission estimate by 8%. Changing the stability classification at a 15 min interval from Pasquill class D neutral to C or E would increase or decrease the emission estimate by 40% respectively. Changing the initial dispersion in the wake of the buildings from 5m to 10 m reduced the emission by 20%. Together the different sensitivity runs result in emission estimates with a standard deviation of 25% around the emission level of 9.2 kg NH_3 d^1.This uncertainty range is probably more accurate compared to the calculated standard errors bases on the large number of observations. The freedom of choice in the input parameters for the model would be reduced significantly with data available on the vertical distribution of NH_3 downwind of the source. Additional data along a vertical profile up to about 10 m height would have provided better constraints on the parameters that set the vertical dispersion in the model.

Table 6 shows the result of a sensitivity analysis on the major parameters that might affect the estimation of the emission strength using the FIDES-2-D model, as well as the effect of taking into account dry deposition downwind of the source. It can be seen that the method using FIDES-2-D is sensitive to the height of the source (h_{src}), the roughness length (z_0), and the size of the source (L_{emi}), and whether deposition is taken into account or not, with a stomatal compensation point (χ_s). A larger source height implies more dispersion of the plume and hence a larger source strength to provide the same concentration. A larger z_0 also induces more dispersion and hence a larger source strength to get the same concentration downwind. A smaller source implies a larger source density but the integrated source is still smaller than for a wider

BGD
6, 825–862, 2009

source. The effect of deposition is straightforward; since NH_3 is deposited, more emission is needed in order to get the same concentration downwind. Increasing χ_s by a small amount does not have a great effect, as the modelled cuticular resistance R_w was small compared to R_s. Combining all the most important effects to maximize the calculated emission within the ranges tested, (h_{src}=5 m, z_0=1.0 m, L_{emi}=400 m, χ_s=0 μg $NH_3 m^{-3}$), one would obtain an increase of 96% of the source strength, giving a daily emission strength of 11.7 kg NH_3 day^1, which is higher than the emission factor estimate of the source. Although this is an extreme test, using all the limits of the uncertainty to favour large emission, the set of parameters is not unrealistic as the source was rather higher than 1 m, the roughness length must be higher tan 0.1 m due to the buildings, and deposition of NH_3 is probable on the canopy upwind from the receptor location. It can thus be concluded that, together with the effect of lateral dispersion, uncertainty in these factors can fully account for the difference between the FIDES-2-D application and other estimates from the Gaussian model and the inventory.

Table 6 shows that deposition as well as the source geometry can really influence the emission strength inferred with inverse modelling techniques. However of these two effects, deposition is probably the more problematic in the case of emissions from farm building, since there is a much larger uncertainty on the deposition parameters (R_s and particularly R_w and χ_s) than on the source geometry. Indeed, the fields in between the source and Site 3 were patches of small crop trials of varying R_s, R_w and χ_s, which makes it difficult to define a unique surface characteristic. Moreover, R_w is a very uncertain parameter that has a major influence on local deposition (e.g., Loubet and Cellier 2002). This constitutes a major uncertainty in the dispersion model approach, which is difficult to overcome. One way would be to perform the measurements closer to the source and at higher levels (such as Welch et al., 2005b). However, the influence of the farm buildings on the flow would prohibits the use of Gaussian-like models, and would require more sophisticated models. This study also suggests that the used of a 3-D model is probably necessary to estimate the emission strength at such distances from a source.

5.2 Daily variability of the emissions from a naturally ventilated building

Figure 4 and 5 show that the emission strength followed a clear diurnal pattern, with a maximum in mid-morning and a minimum at night. Although some of this variability is reflected in the concentration change (Fig. 5), this is not always the case, because of the daily pattern of the turbulent diffusivity. The question arises whether this variability in emission is real or is a bias linked with the inference method. Indeed, the emission from farm houses with forced ventilating systems can be rather constant with time, due to a rather constant indoor temperature regulated by the ventilation system. However, at the FAL farm studied here, most of the buildings are naturally ventilated, which implies that the indoor temperatures fluctuate and that the flow rate through the buildings also changes with environmental conditions (Welch et al., 2005b; Zhang et al., 2005). This seems to be confirmed by Figure 5, where one can see a morning maximum, which might for example be due to a flushing out of NH_3 accumulated during the night.

Figure 6 shows the hourly-mean emission strength as a function of the indoor temperature of the main cattle building (A in Fig. 1). This suggests that the inferred daily variability of the emission strength is real, since NH_3 emission is expected to vary as the exponential function of the temperature according to the Clausius-Clapeyron law (e.g., with a doubling of emission for every 5°C increase, Sutton et al., 2001). This dependence of NH_3 emissions to indoor temperature was experimentally demonstrated by Zhang et al. (2005) over a range of temperature 5–23°C. However Zhang et al. found a maximum increase by a factor of 3 over the range of temperature observed here (14–23°C), whereas Figure 6 shows an increase of up to a factor of 7. On the basis of the solubility equilibria, a factor 4 increase would have been expected. This suggests that the response of Fig. 6 may include effects of temperature as well as correlated effects linked with changes in the ventilation rate.

To better understand the factors that cause the observed daily emission pattern, a free and a forced convection velocity were calculated by adapting Monteith and Unsworth (1990) and Murphy et al. (1977) approaches, respectively. These velocities

were computed as the inverse of the transfer resistance R_b, using u_* as a velocity scale, the difference between indoor and outdoor temperatures, and a characteristic size of the building of 10 m was taken. Although the expressions from Murphy et al. (1977) are not adapted to free and forced convection in buildings, they can give a good qualitative information on the daily variability of the ventilation rate. They are shown in Fig. 7, calculated from hourly averages, along with the source strength, and the resultant convective velocity (the sum of the two). The daily pattern of free convection (7a) shows two *maxima*, one between 4 h and 8 h, and the other around 22 h. This pattern is due to a time de-correlation between the indoor and the outdoor temperatures, which might be explained by the building being heated more rapidly than the air in the morning (because of the solar radiation onto the roof and small ventilation), and a longer decrease at night due to the naturally forced ventilation being small at that time. On the opposite, the modelled forced convection velocity follows directly the daily pattern of u_*.

It can be seen that the resultant convective velocity follows very well the source strength pattern (Fig. 7a). A linear regression between the convective velocity and the emission strength gives an R^2=0.97, which is much larger than the R^2 observed between the indoor temperature and the emission strength (Fig. 6). This demonstrates that the emission pattern observed in Fig. 5 is probably caused by (i) the indoor concentration increasing with indoor temperature, as suggested by Fig. 6, and (ii) the ventilation rate increasing also during the day as resulting from the combination of natural convection (indoor temperature change), and forced convection (external wind).

6 Conclusions

Within the framework of the European GRAMINAE project, an intensive joint field experiment was performed at the FAL research station in Braunschweig (Germany), during May and June 2000. This experiment, summarized in Sutton et al. (2008) has brought together many atmospheric NH_3 concentration measurements techniques located at several sites around a cluster of farm buildings. This gave a great opportunity

to use the measured NH_3 concentration, as well as mobile fast sensor measurements to infer the emission from the farm building with inverse modelling technique. Two models were used, a Gaussian-3-D plume model, and the FIDES-2-D model that can take into account deposition.

The inferred emission strength was on average 6.0 kg d^{-1} NH_3 for the FIDES-2-D model and 9.2 kg d^{-1} NH_3 for the Gaussian plume model. The mobile NH_3 measurements provided valuable data on the horizontal dispersion of the NH_3 plume form the farm houses. These data were used to constrain the dispersion model parameters. Concentration measurements of the vertical distribution of NH_3 that could be used to evaluate the vertical dispersion of the NH_3 plume were not available but are recommended for similar experiments in future.

A sensitivity analysis showed that the inference method was very sensitive to the deposition scheme used, and when a maximum deposition was applied, the farm emission strength could be increased by 45%. The height of the source, its size and the surface roughness were found to influence the emission strength estimates both with the FIDES-2-D and the Gauss model by up to 30%. Taking a set of parameters in the FIDES-2-D model combining the height of the source, its size, the roughness length and the deposition of NH_3 could almost double the source strength (up to 11.7 kg d^{-1} NH_3), indicating that these factors, as well as the effects of cross-wind dispersion, can fully explain the differences between the FIDES-2-D model, and estimates from the Gaussian model and inventory. The source-strength exhibited a clear diurnal cycle with a maximum in the morning (07:00–08:00 GMT) and a minimum at night. This variability can be fully explained by changes in the indoor temperature and the ventilation rate.

In the context of remaining uncertainty in the inventory estimates and lack of independent measurement of NH_3 emissions from the buildings, the present work does not fully validate the approach used. However, the application of dispersion models combined with NH_3 concentrations measured at large distances downwind, provides an approach in close agreement with the inventory, while the possibility of underestimation

using the FIDES-2-D approach demonstrates the need to consider other interacting factors, such as cross-wind dispersion and role of dry deposition between the source and the measurement location.

Acknowledgements. The work presented here was partly funded by the EU FP5 GRAMINAE Project (EU contract ENV4-CT98-0722). Final synthesis of this paper was conducted as part of the NitroEurope Integrated Project We thank the Spanish Commission of Advanced Education and Scientific Research (Dirección General de Enseñanza Superior e Investigación Científica) who provided funding for J. Mosquera to come to the Energy Research Center of the Netherlands (ECN) as a postdoctoral fellow, and the UK Department for Environment Food and Rural Affairs (Defra).

References

Asman, W. A. H.: Ammonia emission in Europe: updated emission and emission variations, Report 228471008, National Institute of Public Health and Environmental Protection (RIVM), Bilthoven, The Netherlands, 1992.

Bobbink, R., Boxman, D., Fremstad, E., Heil, G., Houdijk, A., and Roelofs, J.: Critical loads for nitrogen eutrophication of terrestrial and wetland ecosystems based upon changes in vegetation and fauna, In: Critical loads for nitrogen (edited by: Grennfelt, P. and Thörnelöf, E.), pp. 41, Nordic Council of Ministers, Copenhagen, 1992.

Bouwman, A. F., Lee, D. S., Asman, W. A. H., Dentener, J. F., van de Hoek, K. W., and Olivier, J. J. G.: A global emission inventory for ammonia, Global Biogeochem. Cy., 11, 561–587, 1997.

Bussink, D. W. and Oenema, O.: Ammonia volatilization from dairy farming systems in temperate areas: a review, Nutr. Cycl. Agroecosys., 51, 1352–2310, 1998.

Demmers, T. G. M., Burgess, L. R., Short, J. L., Phillips, V. R., Clark, J. A., and Wathes, C. M.: Ammonia emissions from two mechanically ventilated UK livestock buildings, Atmos. Environ., 33, 107–116, 1999.

Döhler, H., Dämmgen, U., Berg, W., Bergschmidt, A., Brunsch, R., Eurich-Menden, B., Lüttich, M., and Osterburg, B.: Adaptation of the German emission calculation methodology to international guidelines, determination and forecasting of ammonia emissions from German

agriculture, and scenarios for reducing them by 2010 (in German, summary in English), in print at Umweltbundesamt (Berlin), 2002.
Dore, C. J., Jones, B. M. R., Scholtens, R., Huis in'T Veld, J. W. H., Burgess, L. R., and Phillips, V. R.: Measuring ammonia emission rates from livestock buildings and manure stores – Part 2: Comparative demonstrations of three methods on the farm, Atmos. Environ., 38, 3017–3024, 2004.
Erisman, J. W., Otjes, R., Hensen, A., Jongejan, P., v. d. Bulk, P., Khlystov, A., Mols, H., and Slanina, S.: Instrument development and application in studies and monitoring of ambient ammonia, Atmos. Environ., 35, 1913–1922, 2001.
Flesch, T. K., Wilson, J. D., Harper, L. A., and Crenna, B. P.: Estimating gas emissions from a farm with an inverse-dispersion technique, Atmos. Environ., 39, 4863–4874, 2005.
Flesch, T. K., Wilson, J. D., Harper, L. A., Todd, R. W., and Cole, N. A.: Determining ammonia emissions from a cattle feedlot with an inverse dispersion technique, Agr. Forest Meteorol., 144, 139–155, 2007.
Galloway, J. N.: Acid deposition: perspectives in time and space, Water, Air and Soil Pollution, 85, 15–24, 1995.
Gash, J. H. C.: A note on estimating the effect of a limited fetch on micrometeorological evaporation measurements, Bound. Lay. Meteorol., 35, 409–413, 1985.
Heij, G. J. and Schneider, T.: Acidification research in the Netherlands, 3–24, Studies in Environmental Science 46, Elsevier, Amsterdam, 1991.
Heij, G. J. and Schneider, T.: Dutch Priority Programme on Acidification. Final report No. 300–05, National Institute of Public Health and Environmental Protection (RIVM), Bilthoven, The Netherlands, 1995.
Hensen, A. and Scharff, H.: Methane emission estimates from landfills obtained with dynamic plume measurements, Water Air Soil Poll., Kluwer, focus1, 455–464, 2001.
Huang, C. H.: A theory of dispersion in turbulent shear flow, Atmos. Environ., 13, 453–463, 1979.
Jarvis S. C. and Pain, B. F.: Ammonia volatilisation from agricultural land, Proceedings of the Fertiliser Society, 298, 35 pp., The Fertiliser Society, Peterborough, 1990.
Lin, J. S. and Hildemann, L. M.: A Generalized mathematical scheme to analytically solve the atmospheric diffusion equation with dry deposition, Atmos. Environ., 31, 59–71, 1997.
Loubet, B. and Cellier,P.: Experimental assessment of atmospheric ammonia dispersion and short-range dry deposition in a maize canopy, Water Air Soil Poll., 1(5/6), 157–166, 2002.

Loubet, B., Cellier, P., Milford, C., and Sutton, M. A.: A coupled dispersion and exchange model for short-range dry deposition of atmospheric ammonia, Quart. J. Royal. Meteor. Soc., 132, 1733–1763, 2006.

Loubet, B., Milford, C., Sutton, M. A., and Cellier, P.: Investigation of the interaction between sources and sinks of atmospheric ammonia in an upland landscape using a simplified dispersion-exchange model, J. Geophys. Res., 106(D20), 24183–24196, 2001.

Michorius et al., Michorius, J.A.T., Hartog, K. D., Scholtens, R., Harssema, H.: Measuring ammonia emissions from building complexes using the flux frame method and the Gaussian plume model: a feasibility study, IMAG-DLO Report 95-11, Wageningen, The Netherlands, 1997.

Milford, C., Theobald, M. R., Nemitz, E., Hargreaves, K. J., Horvath, L., Raso, J., Dämmgen, U., Neftel, A., Jones, S. K., Hensen, A., Loubet, B., Cellier, P., and Sutton, M. A.: Ammonia fluxes in relation to cutting and fertilization of an intensively managed grassland derived from an inter-comparison of gradient measurements, Biogeosciences Discuss., 5, 4699–4744, 2008, http://www.biogeosciences-discuss.net/5/4699/2008/.

Monteith J. L. and Unsworth M. H.: Principles of Environmental Physics, 2nd ed., 291 pp., Arnold, New York, 1990.

Mosquera, J., Monteny G. J., and Erisman J. W.: Overview and assessment of techniques to measure ammonia emissions from animal houses: the case of the Netherlands, Environ. Pollut., 135, 381–388, 2005.

Nemitz, E., Loubet, B., Cellier, P., Lehmann, B., Neftel, A., Jones, S. K., Hargreaves, K. J. and Sutton M. A.: Turbulence characteristics and transport mechanisms in grassland canopies, Biogeosciences Discuss., accepted, 2008.

Pasquill, F.: Atmospheric Diffusion, 2nd ed., J. Wiley & Sons, New York, 1974.

Pain, B.F., van der Weerden, T. J., Chambers, B. J., Phillips, V. R., and Jarvis, S. C.: A new inventory for ammonia emissions from UK agriculture, Atmos. Environ., 32, 309–313, 1998.

Philip, J. R.: The theory of local advection: 1, J. Meteorol., 16, 535–547, 1959.

Phillips, V. R., Lee, D. S., Scholtens, R., Garland, J. A., and Sneath, R. W.: A review of methods for measuring emission rates of ammonia from livestock buildings and slurry or manure stores, part 2: monitoring flux rates, concentrations and airflow rates, J. Agr. Eng. Res., 78, 1–14, 2001.

Raupach, M. R.: Stand overstorey processes, Philos. Trans. R. Soc., London, Ser. B., 324,

175–190, 1989.
Scholtens, R., Dore, C. J., Jones, B. M. R., Lee, D. S., and Phillips, V. R.: Measuring ammonia emission rates from livestock buildings and manure stores - Part 1: Development and validation of external tracer ratio, internal tracer ratio and passive flux sampling methods, Atmos. Environ., 38, 3003–3015, 2004.
Smith, F. B.: The diffusion of smoke from a continuous elevated point source into a turbulent atmosphere, J. Fluid Mech., 2, 49–76, 1957.
Sommer, S. G., McGinn, S. M., and Flesch, T. K.: Simple use of the backwards Lagrangian stochastic dispersion technique for measuring ammonia emission from small field-plots, Eur. J. Agron., 23, 1–7, 2005.
Sutton, M. A., Nemitz, E., Theobald, M. R., Milford, C., Dorsey, J. R., Gallagher, M. W., Hensen, A., Jongejan, P. A. C., Erisman, J. W., Mattsson, M. E., Schjoerring, J. K., Cellier, P., Loubet, B., Roche, R., Neftel, A., Hermann, B., Jones, S., Lehman, B. E., Horvath, L., Weidinger, T., Rajkai, K., Burkhardt, J., Löpmeier, F. J., and Daemmgen, U.: Dynamics of ammonia exchange with cut grassland: strategy and implementation of the GRAMINAE Integrated Experiment, Biogeosciences Discuss., 5, 3347–3407, 2008, http://www.biogeosciences-discuss.net/5/3347/2008/.
Thomson, D. J.: Criteria for the selection of stochastic models of particle trajectories in turbulent flows, J. Fluid Mech., 180, 529–556, 1987.
Van Breemen, N., Burrough, P. A., Velthorst, E. J., van Dobben, H. F., de Wit, T., Ridder, T. B., and Reijnders, H. F. R.: Soil acidification from ammonium sulphate in forest canopy throughfall, Nature 288, 548–550, 1982.
Welch, D. C., Colls, J. J., Demmers, T. G. M., and Wathes, C. M. A.: Methodology for the measurement of distributed agricultural sources of ammonia outdoors–Part 1: validation in a controlled environment, Atmos. Environ, 39, 663–672, 2005a.
Welch, D. C., Colls, J. J., Demmers, T. G. M., and Wathes C. M.: A methodology for the measurement of distributed agricultural sources of ammonia outdoors - Part 2: Field validation and farm measurements, Atmos. Environ., 39, 673–684, 2005b.
Wilson, J. D., Thurtell, G. W., Kidd, G. E., and Beauchamp, E. G.: Estimation of the rate of gaseous mass transfer from a surface source plot to the atmosphere, Atmos. Environ., 16, 1861–1867, 1982.
Wyers, G. P., Otjes, R. P., and Slanina, J.: A continuous-flow denuder for the measurement of ambient concentrations and surface-exchange fluxes of ammonia, Atmos. Environ., 27A(13),

2085–2090, 1993.
Yeh, G. T. and C. H. Huang: Three-dimensional air pollutant modeling in the lower atmosphere, Bound. Lay. Meteorol., 9, 381–390, 1975.
Zhang, G., Strom, J. S., Li, B., Rom, H. B., Morsing, S., Dahl, P., and Wang, C.: Emission of ammonia and other contaminant gases from naturally ventilated dairy cattle buildings, Biosyst. Eng., 92, 355–364, 2005.

Table 1. Description of the farm animal houses, along with their potential emission estimated using German national emission factors (Döhler et al., 2002) and inventoried number of animals. The total yearly emission of the source is 3.4 10^3 kg year^{-1} NH_3 and the total number of animals is 553. The corresponding average daily total emission is 9.6 kg d^{-1} NH_3.

Source number on map in Fig. 1	Animals	Nr. of animals	Emission factor per animal kg NH_3 animal^{-1} year^{-1}	Emission per building kg NH_3 year^{-1}	Percentage contribution %
A	Cattle	60	10.35	621	18%
B	Cattle	60	10.35	621	18%
C	Cattle	11	10.35	114	3%
D	Cattle	48	10.35	497	14%
E	Bulls	64	3.89	249	7%
F	Cattle	80	10.35	828	24%
G	Calves	60	3.89	233	7%
H	Calves	0	3.89	0	0%
I	Pigs	80	1.97	158	5%
J	Pigs	45	1.97	89	3%
K	Pigs	45	1.97	89	3%
Total	–	553	–	3499	100%

BGD
6, 825–862, 2009

Table 2. Emission estimates using 4 plume transects measured with the fast response sensor (12 June 2000). Uncertainty of the mean is given as standard error.

	Max Dispersion kg NH_3 d^{-1}	Min Dispersion kg $NH_3 d^{-1}$	Average kg $NH_3 d^{-1}$
Plume 1	8.4	6.1	7.3
Plume 2	11.4	9.3	10.4
Plume 3	11.1	9.3	10.2
Plume 4	10.7	10.4	10.6
Inventory			9.6±0.78

Table 3. Source-receptor relation and source estimate obtained with the Gaussian model using the spatial source distribution as obtained using the inventory data.

	Contribution in %										Q kg NH_3 d^{-1}				
	A	B	C	D	E	F	G & H	I	J	K	Mean	St. dev	N	St. error*	Corr (R)
AM1	26	30	3	9	4	13	3	6	2	2	7	4	456	0.19	0.36
AM2	22	26	4	11	6	15	4	7	3	3	10	10	568	0.42	0.30
AM3	18	23	4	10	6	19	5	8	3	4	12	14	459	0.65	0.20
Mean for 3 stations											9.8				

*standard error=st. deviation/sqrt(n)

BGD
6, 825–862, 2009

Table 4. Source-receptor relation and source estimate obtained with the Gaussian model after modification of the spatial distributions of sources with in the farm area.

	Contribution in %										Q kg NH_3 d^{-1}				
	A	B	C	D	E	F	G & H	I	J	K	Mean	St. dev	n	St. error*	Corr (R)
AM1	0	36	17	25	0	0	0	15	1	6	6	4	286	0.24	0.50
AM2	0	29	22	24	0	0	0	18	1	6	10	2	441	0.38	0.49
AM3	0	23	21	19	0	0	0	26	1	11	11	11	396	0.55	0.24
Average for 3 stations											9.2				

*standard error=st. deviation/sqrt(n)

Table 5. Ammonia source-strength estimated with the Gaussian plume model, as compared to that estimated from the emission factors of Döhler et al. (2002). The total amount of ammonia emitted per year estimated using the Gaussian plume model is 3.3 10^3 kg year^{-1} NH_3 as compared to the inventory estimate of 3.5 10^3 kg year^{-1} NH_3. These values correspond to averaged daily emissions of 9.2 kg d^1 NH_3 and 9.6 kg d^{-1} NH_3, respectively.

			Estimated from emission factors (Döhler et al., 2002)		Estimated with the AMANDA measurements (Site 3) and Gaussian model (this study)	
Building (Fig. 1)	Animals	Number of animals	Emission per building kg NH_3 year^{-1}	Percentage contribution %	Emission per building kg NH_3 year^{-1}	Percentage contribution %
A	Cattle	60	621	18%	0	0%
B	Cattle	60	621	18%	729	22%
C	Cattle	11	114	3%	559	17%
D	Cattle	48	497	14%	598	18%
E	Bulls	64	249	7%	0	0%
F	Cattle	80	828	24%	4	0%
G	Calves	60	233	7%	0	0%
H	Calves	0	0	0%	0	0%
I	Pigs	80	158	5%	926	28%
J	Pigs	45	89	3%	43	1%
K	Pigs	45	89	3%	483	14%
Total		553	3499	100%	3341	100%

Table 6. Daily emission of the source estimated using the emission factor and the modelling approach, and sensitivity of each estimate to micrometeorological parameters. Standard parameters used were: h_{src}=1.0 m, z_0= 0.057 m, Source width=180 m, and no dry deposition. In the sensitivity analysis, h_{src} have been set to 0 and 5 m height, z_0 has been set to 0.01 m and 1.0 m, the source width has been set to 50 and 400 m, and in the deposition sensitivity analysis, the stomatal compensation point χ_s has been set to 0 and 1 μg m^{-3} NH_3. The cuticular R_w and stomatal resistance R_s were estimated as R_w=7exp$^{((100-RH)/12)}$, and R_s=30 ×1+200/max(0.01, St), where RH is the relative humidity at z_0' and St is the global solar radiation.

Methodology	Daily emission	Sens. to h_{src} (0–5 m)	Sens. to z_0 (0.01–1.0 m)	Source width L_{emi} (50–400 m)	With deposition χ_s (0–2 μg m^{-3}NH_3)
	kg d^{-1}NH_3	kg d^{-1} NH_3	kg d^{-1} NH_3	kg d^{-1} NH_3	kg d^{-1} NH_3
Emission factors	9.6	-	-	-	-
Inverse FIDES	6.0 ± 3.8	5.8–7.2	5.6–7.4	4.9–7.6	8.7–8.5
		%	%	%	%
Percentage		-4% - +20%	-6% - +23%	-19% - +27%	45% - 41%

BGD
6, 825–862, 2009

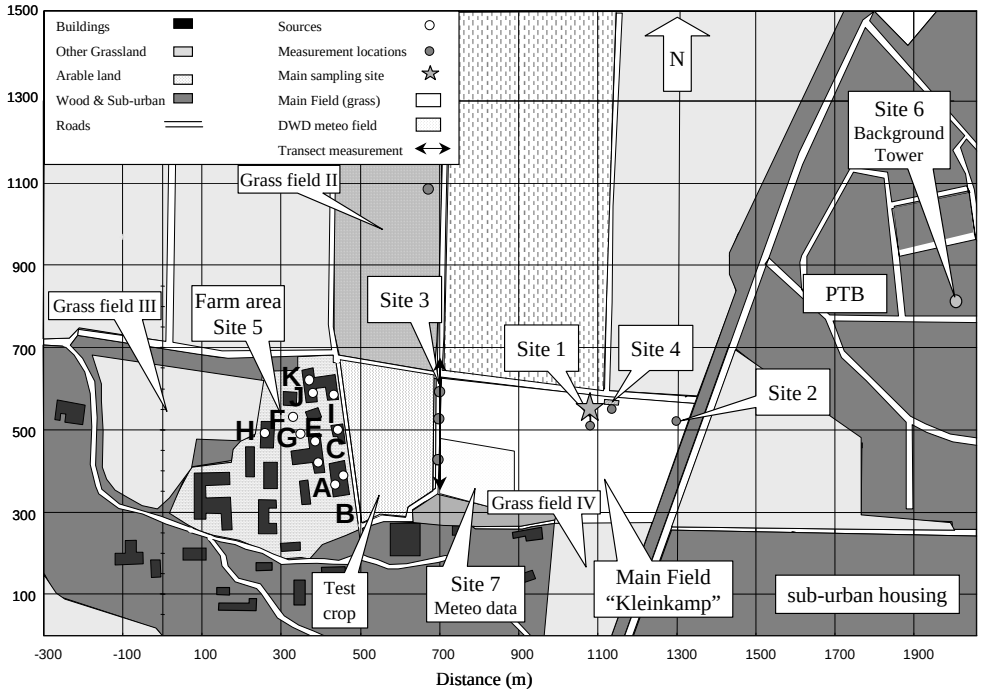

Fig. 1. Overview of the measurement site. The three locations of NH_3 air concentration measurement (grey circles) used in this analysis are indicated as Site 1, Site 2 and Site 3. The plume transect measurements were made along the track at Site 3. The sources buildings are labelled from A to K (see Table 1). Distances are shown on the axes of the map in meters (For further description of the site, see Sutton et al., 2008.

BGD
6, 825–862, 2009

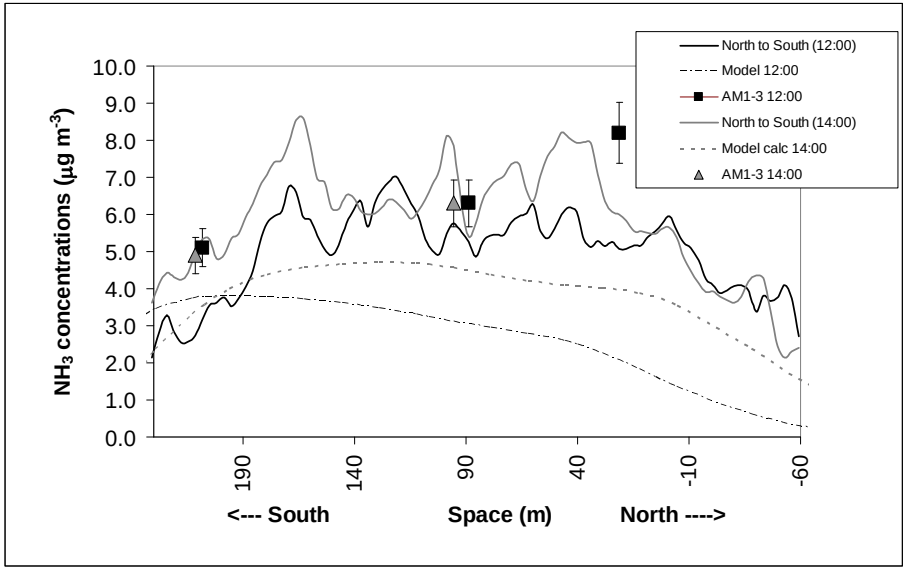

Fig. 2. Two fast-sensor measurements of the NH_3 plume cross-section at Site 3 the 12/06/2000 at 12:00 and 14:00. The simultaneous concentrations measurements obtained with the 3 stationary AMANDA systems ($AM_{1..3}$) are shown at their corresponding locations in the plume. The figure also shows the plume modeled with the Gaussian-3-D model using the source distribution and strength as given in Table 1. The difference between the fast sensor and the stationary AMANDA concentrations is mainly due to the time response of the AMANDA being 15 min while the fast sensor has a 30 time response. For the N-S axis, 0 m corresponds to the intersection with the main E-W track N of Kleinkamp (Fig.1).

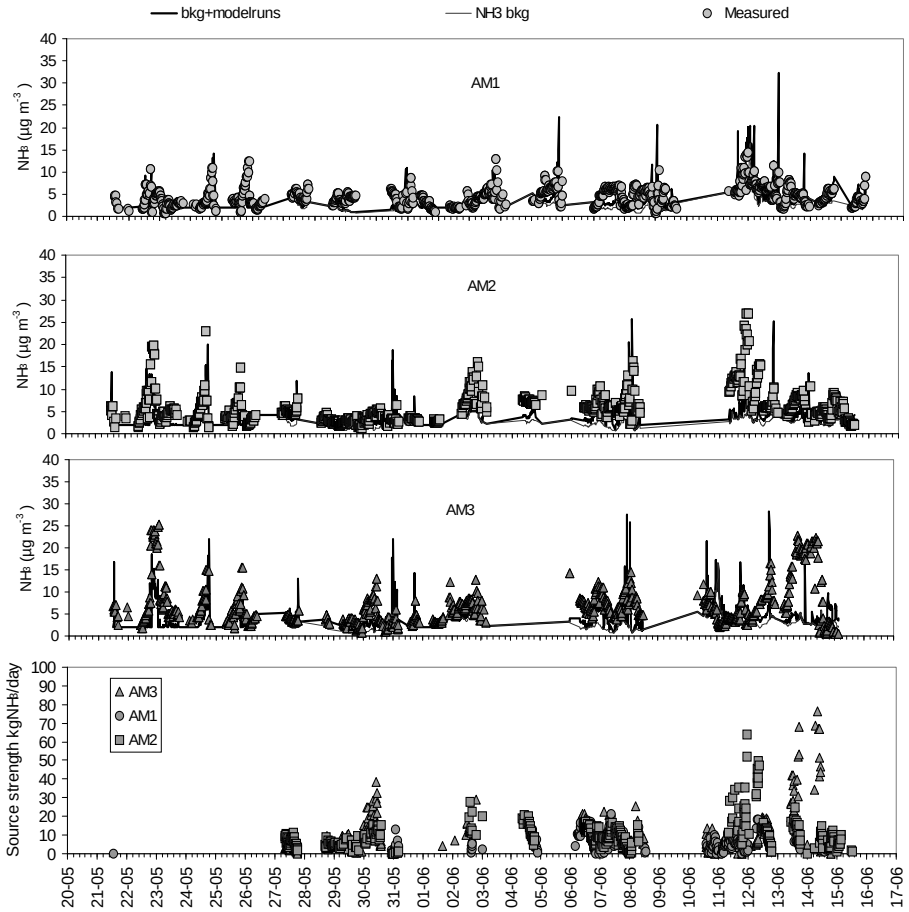

Fig. 3. Example of measured and modeled concentration with the Gaussian plume model by AM1-3 at Site 3. The source-strengths of the farm buildings were estimated by minimizing the difference between the measured and the modeled concentrations at all locations.

BGD
6, 825–862, 2009

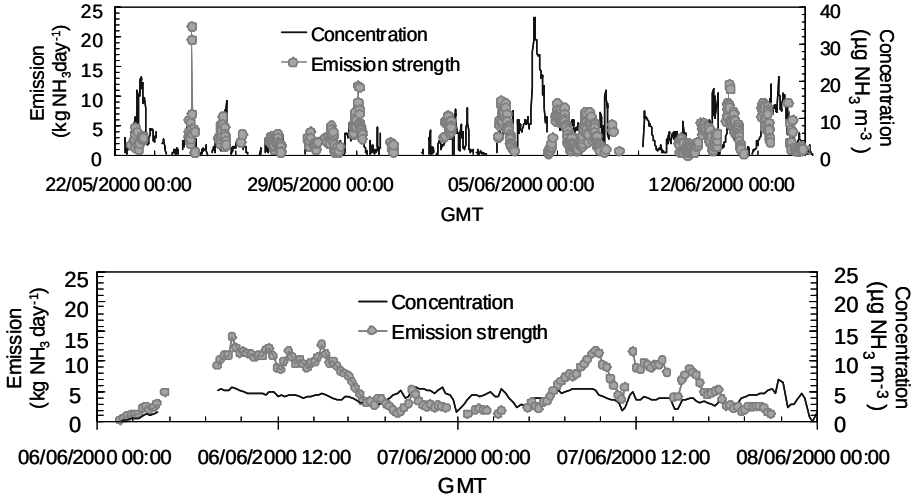

Fig. 4. (top graph) time course of the NH_3 emission strength as inferred with the FIDES-2-D model using the averaged concentration measured for the wind direction 240°–300°at Site 3 and the background concentration measured at Site 6. Also shown is the concentration difference Site 3–Site 6. (bottom graph) magnification for the period 6–8 June.

BGD
6, 825–862, 2009

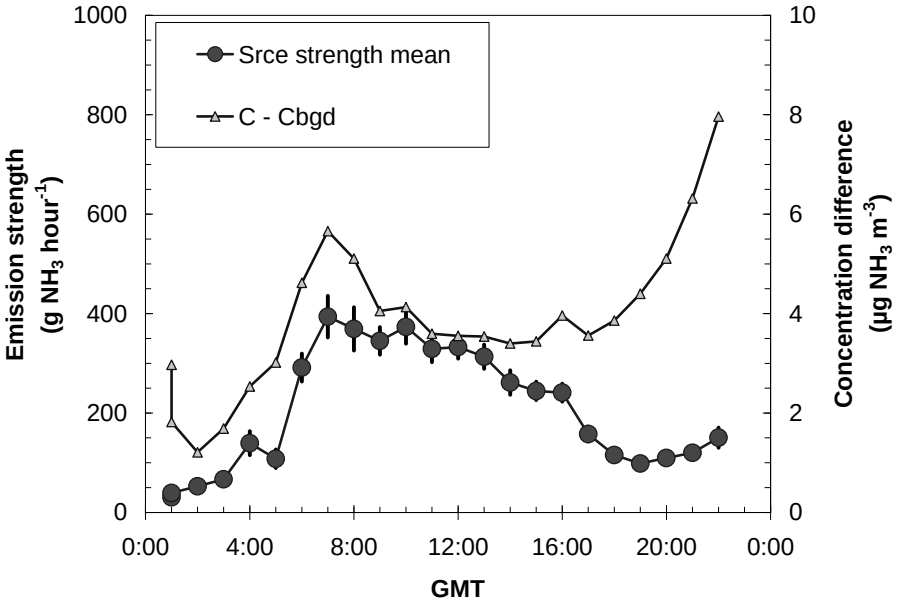

Fig. 5. Diurnal variability of the farm NH_3 source strength as estimated with the FIDES-2-D model for a wind sector of 240°–300°. The concentration difference between Site 3 and the background at Site 6 ($C\text{-}C_{bgd}$) is also given. The dark circles represent the source strength during the whole period that has been hourly averaged to give the mean source strength for each hour. The error bars are the standard errors.

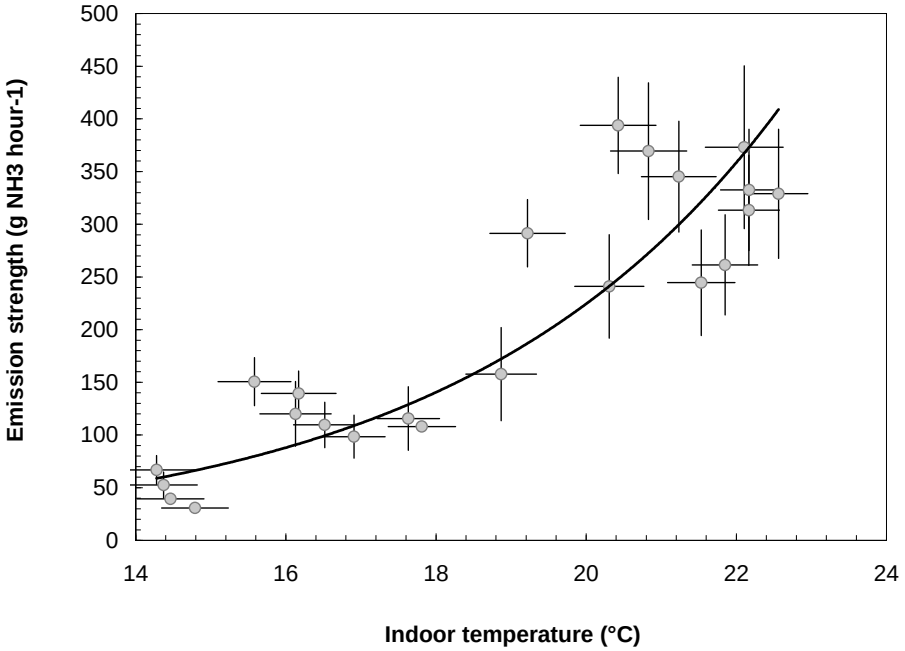

Fig. 6. Hourly averaged emission strength for a wind sector of 240°–300° as a function of hourly mean indoor temperature (measured for the main cattle building A). The bold line is a regression with equation: Srce [g h^{-1} NH_3]=2.1exp(0.2341×T[K]–63.94), R^2=0.82. The error-bars are ± standard deviation.

BGD
6, 825–862, 2009

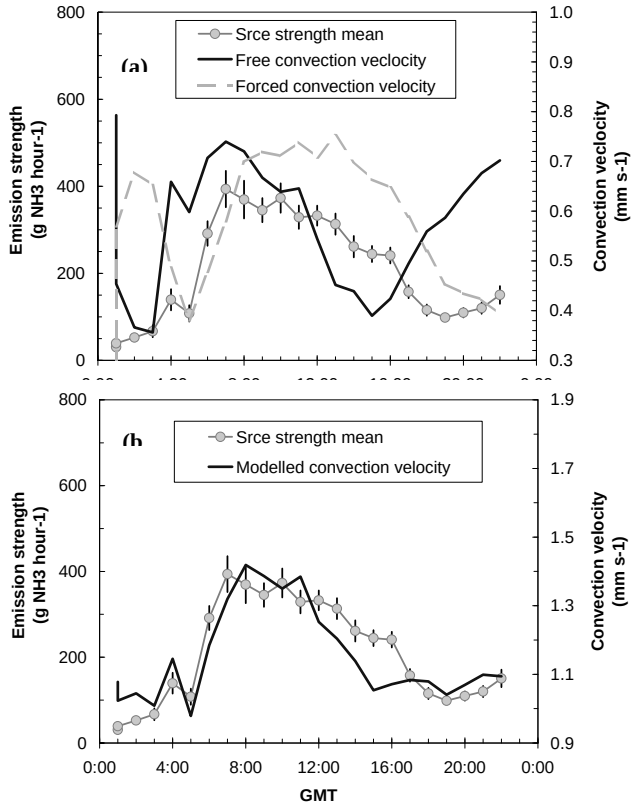

Fig. 7. Hourly averaged emission strength for a wind sector of 240°–300°, **(a)** free and forced convection velocities calculated as $1/R_b$, and **(b)** resultant total convection velocity (sum of free and forced convection velocities). The error-bars are ± standard errors. A linear regression between the convection velocity and the emission strength gives an R^2=0.97.

BGD
6, 825–862, 2009